Temperature dependence of hybridization gaps in metallic heavy-fermion systems

2011 J. Phys.: Condens. Matter 23 094211

(http://iopscience.iop.org/0953-8984/23/9/094211)

IOP Publishing Journal of Physics: Condensed Matter

J. Phys.: Condens. Matter **23** (2011) 094211 (7pp) doi:10.1088/0953-8984/23/9/094211

Temperature dependence of hybridization gaps in metallic heavy-fermion systems

Xiaodong Yang[1], Peter S Riseborough[1] and Tomasz Durakiewicz[2]

[1] Physics Department, Temple University, USA
[2] MPA-CMMS, Los Alamos National Laboratory, Los Alamos, NM, USA

Received 12 July 2010, in final form 24 August 2010
Published 17 February 2011
Online at stacks.iop.org/JPhysCM/23/094211

Abstract

There is evidence that a number of heavy-fermion/mixed-valence materials show hybridization gaps either at the Fermi energy or close to it. In the former case, a heavy-fermion semiconducting state ensues, and in the latter case, the system remains metallic at low temperatures. In either case, there are significant indications that the electronic structure is extremely temperature dependent. In particular, there is evidence from spectroscopic and transport properties that the gap closes at high temperatures and also that the heavy-quasiparticle bands disappear at high temperatures. The magnitudes of the gaps scale with the effective quasiparticle masses. We present a phenomenological model that exhibits a temperature dependence which is consistent with the above behavior. The model is based on a periodic array of Anderson impurities in which the electron correlations are represented by the coupling to bosons with Einstein spectra. The model can be approximately solved in a systematic manner. The solution consists of semi-analytic expressions which represent the temperature dependences of the coherent and incoherent structures in the electronic excitation spectra. We shall compare the hybridization gaps predicted by the theory for the metallic case and those inferred from photoemission experiments on UPd_2Al_3.

(Some figures in this article are in colour only in the electronic version)

1. Introduction

Many heavy-fermion materials exhibit hybridization gaps in their electronic spectra. In the case where the chemical potential lies within the hybridization gap, the ground state is a heavy-fermion semiconductor [1, 2] or Kondo insulator. The indirect hybridization gap can be extracted from the temperature dependence of the transport properties [3] as the activation energy, or can be inferred from spectroscopic measurements such as photoemission [4, 5] or inelastic neutron scattering experiments [6, 7]. The direct gap can be inferred from optical absorption measurements [8–10]. When the chemical potential lies outside the hybridization gap, either metallic or semi-metallic [11–13] behavior results. There is evidence that the hybridization gaps in the heavy-fermion semiconductors close as the temperature is increased, which is in accordance with slave boson theories [7]. However, whereas in the mean-field slave boson description the gap falls to zero above the coherence temperature, in some experiments on cerium compounds the gap was found to remain finite but small at the highest temperatures [14]. Hybridization gaps in the density of states have also been observed in metallic systems at sufficiently low temperatures. In the metallic case, the magnitude of the hybridization gap follows a simple universal scaling with the quasiparticle effective mass [10]. The metallic uranium compound UPd_2Al_3 lies directly on the scaling line and other systems, such as either URu_2Si_2 [15] or UPt_3 [16], deviate slightly from the linear relationship, perhaps either due to an enhancement of effective mass by magnetic excitations or due to the suppression of the hybridization gap by magnetic ordering. Our photoemission measurements of UPd_2Al_3, discussed below, indicate that in spite of the magnetic ground state, the low temperature value of the gap follows the universal scaling law and temperature dependence of the hybridization gap follows the mean-field behavior.

In this paper, we shall provide a phenomenological theory which describes the temperature dependence of the hybridization gap in semiconducting and metallic systems based on an electron–boson coupling interaction. The coherent part of the hybridization which produces the gap is found to be subject to an exponential renormalization that is reduced as the temperature is increased. The remaining

part of the self-energy is responsible for the scattering of the quasiparticles, and is minimal at the Fermi energy and increases as the temperature is increased. In what follows, we shall describe the model Hamiltonian and perform a canonical transformation that mixes the electronic and bosonic degrees of freedom. We shall calculate the single-fermion f Green's function, and determine the temperature dependence of the hybridization gap for the metallic case and compare our results with the temperature dependence of the gap extracted from photoemission experiments on UPd_2Al_3.

2. The model Hamiltonian

The model Hamiltonian is based on the non-interacting Anderson Lattice model which describes hybridized f and conduction bands. The electronic correlations are modeled by a bath of bosons which are coupled to the f electronic system via an interaction linear in the boson displacement. The total Hamiltonian is written as

$$\begin{aligned}\hat{H} = &\sum_{i,\sigma} E_{\rm f} f^{\dagger}_{i\sigma} f_{i\sigma} + \sum_{\underline{k},\sigma} \epsilon_{\underline{k}} d^{\dagger}_{\underline{k}\sigma} d_{\underline{k}\sigma} \\ &+ \sum_{\underline{k},\sigma}\left(V_{\underline{k}} f^{\dagger}_{\underline{k}\sigma} d_{\underline{k}\sigma} + V^{*}_{\underline{k}} d^{\dagger}_{\underline{k}\sigma} f_{\underline{k}\sigma}\right) \\ &+ \sum_{\underline{q}} \hbar\omega_{\underline{q}} a^{\dagger}_{\underline{q}} a_{\underline{q}} + \sum_{\underline{k},\sigma,\underline{q}} \lambda_{\underline{q}}\left(a^{\dagger}_{\underline{q}} + a_{-\underline{q}}\right) f^{\dagger}_{\underline{k}+\underline{q}\sigma} f_{\underline{k}\sigma}. \end{aligned} \tag{1}$$

The first term represents the binding energy $E_{\rm f}$ of the localized f states at the lattice sites labeled by the index i. Here, the operators $f^{\dagger}_{i\sigma}$ and $f_{i\sigma}$, respectively, create and annihilate an f electron of spin σ in the orbital located at site i. The second term represents the energy $\epsilon_{\underline{k}}$ of the conduction band Bloch states labeled by the Bloch wavevector $\underline{k}$, and $d^{\dagger}_{\underline{k}\sigma}$ and $d_{\underline{k}\sigma}$, respectively, create and annihilate a conduction electron of spin σ in the $\underline{k}$th Bloch state. The third term represents the hybridization between the localized f electron states and the conduction band states. The fourth term represents the energy $\hbar\omega_{\underline{q}}$ of a boson in the bath labeled by the wavevector $\underline{q}$, in which $a^{\dagger}_{\underline{q}}$ and $a_{\underline{q}}$ are, respectively, the boson creation and annihilation operators. The last term represents the interaction between the f electrons and the boson bath.

The bosonic degrees of freedom can be thought as emulating the slave bosons which represent the effect of the electron–hole excitations of the system in the limit of a large Coulomb interaction strength. In the Kondo limit appropriate to nonmagnetic Ce compounds, a typical slave boson energy would be around 2 eV. On the other hand, for systems close to magnetic instabilities, the bosonic degrees of freedom can be thought of as describing the incoherent spin fluctuations, where a typical boson energy would be a small fraction of an electronvolt.

2.1. The non-interacting limit

In the limit of non-interacting electrons, i.e. $\lambda_{\underline{q}} \equiv 0$, the electronic structure decouples from the bosons. The electronic part of the non-interacting Hamiltonian $\hat{H}_0$ is given by

$$\hat{H}_0 = \sum_{\underline{k},\sigma}\left(E_{\rm f} f^{\dagger}_{\underline{k}\sigma} f_{\underline{k}\sigma} + \epsilon_{\underline{k}} d^{\dagger}_{\underline{k}\sigma} d_{\underline{k}\sigma} + V_{\underline{k}} f^{\dagger}_{\underline{k}\sigma} d_{i\sigma} + V^{*}_{\underline{k}} d^{\dagger}_{\underline{k}\sigma} f_{\underline{k}\sigma}\right) \tag{2}$$

which is diagonal in the Bloch index. The phase of the hybridization matrix elements can be gauged away by absorbing the phase in either the d or f electron operators. The non-interacting Hamiltonian can then be diagonalized by introducing a pair of new fermionic operators $\alpha_{\underline{k}\sigma}$, $\beta_{\underline{k},\sigma}$, via the canonical transformation

$$\begin{aligned}\alpha_{\underline{k}\sigma} &= f_{\underline{k}\sigma}\cos\Theta_{\underline{k}} + d_{\underline{k}\sigma}\sin\Theta_{\underline{k}} \\ \beta_{\underline{k}\sigma} &= -f_{\underline{k}\sigma}\sin\Theta_{\underline{k}} + d_{\underline{k}\sigma}\cos\Theta_{\underline{k}}\end{aligned} \tag{3}$$

where $\Theta_{\underline{k}}$ is still to be determined. Since the transformation is canonical, the new fermion operators must satisfy the anti-commutation relations;

$$\begin{aligned}\{\alpha_{\underline{k}\sigma}\alpha^{\dagger}_{\underline{k}'\sigma'}\}_{+} = \delta_{\underline{k}\underline{k}'}\delta_{\sigma,\sigma'} \qquad \{\beta_{\underline{k}\sigma}\beta^{\dagger}_{\underline{k}'\sigma'}\}_{+} = \delta_{\underline{k}\underline{k}'}\delta_{\sigma\sigma'} \\ \{\alpha_{\underline{k}\sigma}\beta^{\dagger}_{\underline{k}'\sigma'}\}_{+} = 0.\end{aligned} \tag{4}$$

For the choice of $\Theta_{\underline{k}}$ given by

$$\begin{aligned}\cos 2\Theta_{\underline{k}} &= \frac{E_{\rm f} - \epsilon_{\underline{k}}}{\sqrt{(E_{\rm f}-\epsilon_{\underline{k}})^2 + 4V_k^2}} \\ \sin 2\Theta_{\underline{k}} &= \frac{2V_k}{\sqrt{(E_{\rm f}-\epsilon_{\underline{k}})^2 + 4V_k^2}}\end{aligned} \tag{5}$$

the terms in the Hamiltonian which are bi-linear in the fermion operators α and β vanish. For this choice of $\Theta_{\underline{k}}$, the non-interacting electronic Hamiltonian has the diagonal form

$$\begin{aligned}\hat{H}_0 = &\sum_{\underline{k},\sigma}\left(\frac{E_{\rm f}+\epsilon_{\underline{k}}}{2} + \sqrt{\left(\frac{E_{\rm f}-\epsilon_{\underline{k}}}{2}\right)^2 + V_k^2}\right)\alpha^{\dagger}_{\underline{k}\sigma}\alpha_{\underline{k}\sigma} \\ &+ \sum_{\underline{k},\sigma}\left(\frac{E_{\rm f}+\epsilon_{\underline{k}}}{2} - \sqrt{\left(\frac{E_{\rm f}-\epsilon_{\underline{k}}}{2}\right)^2 + V_k^2}\right)\beta^{\dagger}_{\underline{k}\sigma}\beta_{\underline{k}\sigma}.\end{aligned} \tag{6}$$

The electronic dispersion relations are shown in figure 1. We note that the spectrum exhibits a direct gap between the pair of hybridized bands of energy 2 V and an indirect gap given by $\Delta = \frac{4V^2}{W}$, where W is the conduction band width. It is the hybridization gap Δ which plays an important role in the description of heavy-fermion semiconductors, and is responsible for the gap seen in the photoemission spectra of metallic heavy-fermion systems.

3. The canonical transformation

The mass enhancement of the f quasiparticle excitations in the metallic limit may be understood if one assumes that the hybridization matrix elements are subjected to a polaronic reduction. This can be achieved by using a canonical transformation which is a variant of the Lee–Low–Pines transformation [17] that is given by

$$\hat{U} = \exp\left[-\frac{1}{\sqrt{N}}\sum_{\underline{q},j,\sigma}\frac{\lambda_{\underline{q}}}{\hbar\omega_{\underline{q}}}(a^{\dagger}_{\underline{q}} - a_{-\underline{q}}) f^{\dagger}_{j,\sigma} f_{j,\sigma}\exp[i\underline{q}\cdot\underline{R}_j]\right]. \tag{7}$$

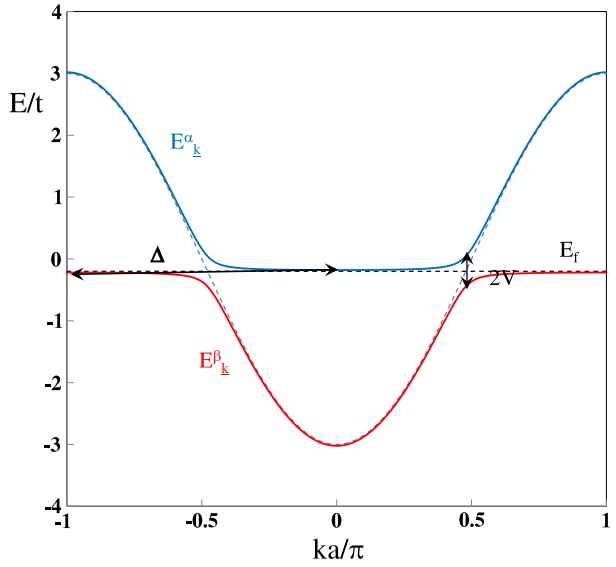

Figure 1. A sketch of the dispersion relations for the non-interacting hybridized electronic bands. The system exhibits an indirect band gap of $\Delta = \frac{4V^2}{W}$ and a direct gap of $2V$. The direct and indirect gap excitations are depicted by the double headed arrows.

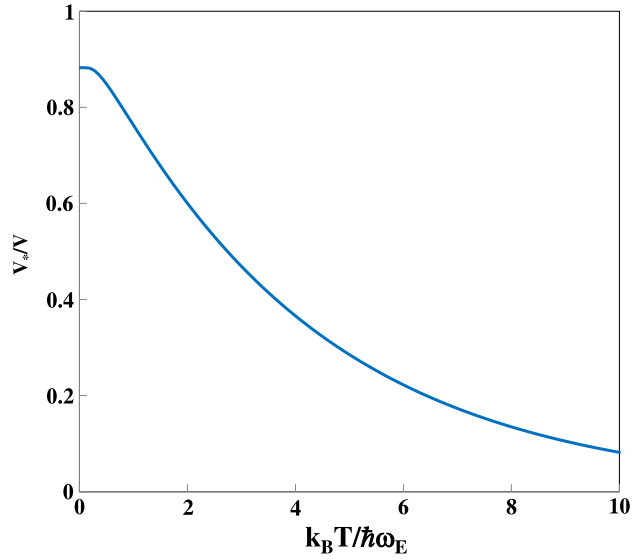

Figure 2. The temperature dependence of the polaronic renormalization of the hybridization matrix element V_*/V. The average number of bosons involved in the distortion at $T = 0$ is given by $\bar{n} = 0.25$.

Applying the transformation to the parts of the Hamiltonian which couple to the bosons, one can eliminate the electron–boson coupling since

$$\hat{H}_b' = \widehat{U}^{\dagger}\Bigg(\sum_{\underline{q}} \hbar\omega_{\underline{q}} a^{\dagger}_{\underline{q}} a_{\underline{q}} + \frac{1}{\sqrt{N}} \times \sum_{\underline{q},\underline{k},\sigma} \lambda_{\underline{q}} (a^{\dagger}_{\underline{q}} + a_{-\underline{q}}) f^{\dagger}_{\underline{k},\sigma} f_{\underline{k}-\underline{q},\sigma}\Bigg)\widehat{U}$$
$$= \sum_{\underline{q}} \hbar\omega_{\underline{q}} a^{\dagger}_{\underline{q}} a_{\underline{q}} - \frac{1}{N} \sum_{\underline{q},\underline{k},\sigma,\underline{k}',\sigma'} \left(\frac{\lambda^2_{\underline{q}}}{\hbar\omega_{\underline{q}}}\right) \times f^{\dagger}_{\underline{k}-\underline{q},\sigma} f_{\underline{k},\sigma} f^{\dagger}_{\underline{k}'+\underline{q},\sigma'} f_{\underline{k}',\sigma'}. \quad (8)$$

Thus, the Hamiltonian is diagonal in the limit $V \to 0$, in which case, the linear electron–boson coupling is removed but in the process, produces a Frank–Condon shift of the f level and also produces an oscillatory long-ranged interaction between the f electrons which, when on-site, reduces to a negative U interaction [18, 19]. In what follows, we shall ignore the interaction between the quasiparticles which is consistent with our neglect of the direct Coulomb interaction U. The canonical transformation has the effect of producing a dynamic renormalization of the hybridization term to yield

$$H_V' = \sum_{j,\underline{k},\sigma}\Bigg(V \exp[i\underline{k}\cdot\underline{R}_j] f^{\dagger}_{j,\sigma} d_{\underline{k},\sigma} \times \exp\Bigg[-\frac{1}{\sqrt{N}}\sum_{\underline{q}} \frac{\lambda_{\underline{q}}}{\hbar\omega_{\underline{q}}}(a^{\dagger}_{\underline{q}} - a_{-\underline{q}}) \exp[i\underline{q}\cdot\underline{R}_j]\Bigg] + \text{H.c.}\Bigg). \quad (9)$$

If this is replaced by the thermal average, as in the Gutzwiller approximate treatment of electronic correlations, one recovers a polaronic reduction of the effective hybridization interaction of the form

$$V \to V_* = V \exp\Bigg[-\frac{1}{2N}\sum_{\underline{q}}\left(\frac{\lambda_{\underline{q}}}{\hbar\omega_{\underline{q}}}\right)^2 (1 + 2\,N_{\underline{q}})\Bigg]. \quad (10)$$

Diagrammatically, the renormalization corresponds to the simultaneous emission and absorption of an indefinite number of bosons at each hybridization vertex. On summing the infinite series, one finds that the series exponentiates, giving rise to the renormalization expressed by equation (10). The temperature dependence of the renormalized hybridization matrix element is similar to that found in Holstein's treatment of the small polaron [20]. The temperature dependence is shown in figure 2.

4. The f electron self-energy

In what follows, we are primarily interested in the temperature dependence of the hybridization gap exhibited in the electronic excitation spectra. If one expresses the single-electron f Green's function in terms of the canonically transformed operators, the f electron creation and annihilation operators must be associated with exponentially factors representing the creation or destruction of distortions in the bosonic bath (similar to the exponential factors shown in equation (9)). Therefore, the f electron Green's function involving the transformed f electron operators should also be expressed in terms of convolutions of f quasiparticle Green's functions (which are defined solely in terms of the f quasiparticle operators) and the boson propagators. Since we are primarily interested in the temperature dependence of the hybridization gap and not the detailed line shapes of the electronic spectra, we shall examine the quasiparticle Green's function which is devoid of the exponential operators that distort the bosonic bath. The interactions in the model can be

completely subsumed in the self-energy for the f electrons. We shall expand the self-energy in powers of the dynamical hybridization vertices. The lowest-order contribution to the self-energy is of order V^2. The dynamic hybridization can be expanded in powers of the electron–boson coupling. The resulting diagrams contain a number of bosons that are emitted and absorbed at just one vertex and bosons that propagate between adjacent vertices. The infinite set of diagrams with the same number of bosons propagating between adjacent vertices can be summed over exactly, and lead to the polaronic renormalization of both vertices. The self-energy is given by the sum of a coherent part and the incoherent part

$$\Sigma_{\rm f}(\underline{k},\omega) = \frac{|V_*|^2}{\hbar\omega - \epsilon_{\underline{k}} + \mu} + \Sigma_{\rm f}^{\rm inc}(\underline{k},\omega) \tag{11}$$

where, to order ${V_*}^2$, the incoherent part of the self-energy is given by

$$\begin{aligned}\Sigma_{\rm f}^{\rm inc}(\underline{k},\omega) \approx{}& \frac{|V_*|^2}{N}\sum_{\underline{q}}\left(\frac{\lambda_{\underline{q}}}{\hbar\omega_{\underline{q}}}\right)^2 \\ &\times\left[\frac{N_{\underline{q}} + f_{\underline{k}-\underline{q}}}{\hbar\omega - \epsilon_{\underline{k}-\underline{q}} + \mu + \hbar\omega_{\underline{q}}} + \frac{1 + N_{\underline{q}} - f_{\underline{k}-\underline{q}}}{\hbar\omega - \epsilon_{\underline{k}-\underline{q}} + \mu - \hbar\omega_{\underline{q}}}\right] \\ &+ \frac{|V_*|^2}{2N^2}\sum_{\underline{q},\underline{q}_1,\underline{q}_2}\left(\frac{\lambda_{\underline{q}_1}}{\hbar\omega_{\underline{q}_1}}\right)^2\left(\frac{\lambda_{\underline{q}_2}}{\hbar\omega_{\underline{q}_2}}\right)^2\delta_{\underline{q}-\underline{q}_1-\underline{q}_2} \\ &\times\left[\frac{f_{\underline{k}-\underline{q}}(1+N_{\underline{q}_1}+N_{\underline{q}_2}) + N_{\underline{q}_1}N_{\underline{q}_2}}{\hbar\omega - \epsilon_{\underline{k}-\underline{q}} + \mu + \hbar\omega_{\underline{q}_1} + \hbar\omega_{\underline{q}_2}}\right. \\ &+ \frac{f_{\underline{k}-\underline{q}}(N_{\underline{q}_1} - N_{\underline{q}_2}) + N_{\underline{q}_2}(1+N_{\underline{q}_1})}{\hbar\omega - \epsilon_{\underline{k}-\underline{q}} + \mu - \hbar\omega_{\underline{q}_1} + \hbar\omega_{\underline{q}_2}} \\ &+ \frac{f_{\underline{k}-\underline{q}}(N_{\underline{q}_2} - N_{\underline{q}_1}) + N_{\underline{q}_1}(1+N_{\underline{q}_2})}{\hbar\omega - \epsilon_{\underline{k}-\underline{q}} + \mu + \hbar\omega_{\underline{q}_1} - \hbar\omega_{\underline{q}_2}} \\ &\left.+ \frac{(1-f_{\underline{k}-\underline{q}})(1+N_{\underline{q}_1}+N_{\underline{q}_2}) + N_{\underline{q}_1}N_{\underline{q}_2}}{\hbar\omega - \epsilon_{\underline{k}-\underline{q}} + \mu - \hbar\omega_{\underline{q}_1} - \hbar\omega_{\underline{q}_2}}\right] + \ldots. \end{aligned} \tag{12}$$

On integrating the imaginary part of the general nth-order term in the incoherent part of the self-energy, $\Sigma_{\rm f}^{(n)}(\underline{k},\omega)$, over ω, the summation over momenta become completely decoupled. The result is

$$\begin{aligned}&\hbar\int_{-\infty}^{\infty} {\rm d}\omega\, {\rm Im}\,\Sigma_{\rm f}^{(n)}(\underline{k},\omega) \\ &= \frac{\pi|V_*|^2}{n!}\left(\frac{1}{N}\sum_{\underline{q}}\left(\frac{\lambda_{\underline{q}}}{\hbar\omega_{\underline{q}}}\right)^2[1+2N_{\underline{q}}]\right)^n. \end{aligned} \tag{13}$$

On summing over all n, the total weight is found to be given by $\pi|V|^2$ involving the unrenormalized hybridization matrix elements, as would have been found without performing the unitary transformation. From this one sees that the number of virtual bosons involved in the ω integrated spectral weight of the imaginary part of the nth-order term in the self-energy follows a Poisson distribution in which the average number of boson excitations involved $\bar{n}$ is given by

$$\bar{n} = \frac{1}{N}\sum_{\underline{q}}\left(\frac{\lambda_{\underline{q}}}{\hbar\omega_{\underline{q}}}\right)^2[1+2N_{\underline{q}}]. \tag{14}$$

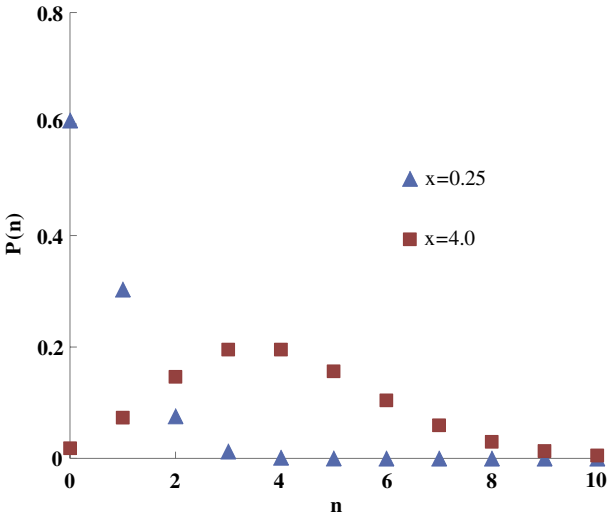

Figure 3. The Poisson distribution $P(n)$ of the number of bosons n involved in the self-energy, for an average number of bosons $\bar{n}$ defined by equation (14) of 0.25 and 4.0.

The Poisson distribution, shown in figure 3, indicates the number of terms that need to be retained in order to calculate the self-energy to a specified accuracy. The number of terms required is expected to increase as the temperature is increased, which is due to the presence of thermally activated bosons. On assuming an Einstein spectrum for the boson, the general nth term in the series for the self-energy $\Sigma_{\rm f}^{(n)}(\underline{k},\omega)$, can be expressed as

$$\begin{aligned}\Sigma_{\rm f}^{(n)}(\underline{k},\omega) ={}& \sum_{\underline{q}}\delta_{(\underline{q}-\sum_{i=1}^n\underline{q}_i)}|V_*|^2\sum_{m=0}^{n}\frac{1}{(n-m)!m!} \\ &\times\left[\left\{f_{\underline{k}-\underline{q}}\left(\frac{1}{N}\sum_{\underline{q}_i}\left(\frac{\lambda_{\underline{q}_i}}{\hbar\omega_E}\right)^2[1+N(\omega_E)]\right)^{n-m}\right.\right. \\ &\left.\times\left(\frac{1}{N}\sum_{\underline{q}_j}\left(\frac{\lambda_{\underline{q}}}{\hbar\omega_E}\right)^2 N(\omega_E)\right)^m\right\} \\ &\times\{\hbar\omega - \epsilon_{\underline{k}-\underline{q}} + \mu - (2m-n)\hbar\omega_E\}^{-1} \\ &+\left\{(1-f_{\underline{k}-\underline{q}})\left(\frac{1}{N}\sum_{\underline{q}_i}\left(\frac{\lambda_{\underline{q}_i}}{\hbar\omega_E}\right)^2 N(\omega_E)\right)^{n-m}\right. \\ &\times\left(\frac{1}{N}\sum_{\underline{q}_j}\left(\frac{\lambda_{\underline{q}_j}}{\hbar\omega_E}\right)^2[1+N(\omega_E)]\right)^m\Big\} \\ &\left.\times\{\hbar\omega - \epsilon_{\underline{k}-\underline{q}} + \mu - (2m-n)\hbar\omega_E\}^{-1}\right]. \end{aligned} \tag{15}$$

The Krönecker delta function expresses conservation of momentum, modulo reciprocal lattice vectors $\underline{Q}$. The delta function can be expressed as

$$\delta_{(\underline{q}-\sum_{i=1}^n\underline{q}_i)} = \frac{1}{N}\sum_{\underline{R}}\exp\left[{\rm i}\left(\underline{q} - \sum_{i=1}^{n}\underline{q}_i\right)\cdot\underline{R}\right] \tag{16}$$

where the sum runs over all the Bravais lattice vectors $\underline{R}$. The self-energy can be evaluated approximately by just retaining

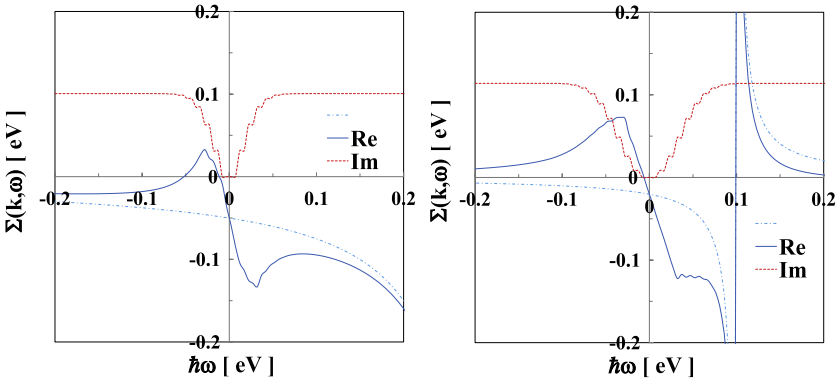

Figure 4. The frequency dependence of the real (solid line) and imaginary (dotted line) parts of the zero-temperature limit of the total self-energy $\Sigma_{\rm f}(k,\omega)$ for $\bar{n}=2$ and $\epsilon_k-\mu=0.3$ (left panel) and for $\bar{n}=4$ and $\epsilon_k-\mu=0.1$ (right panel). The zeroth-order (coherent) term of the self-energy is shown by the dash-dotted lines, and has a simple pole at $\hbar\omega=\epsilon_k-\mu$.

the term with $\underline{R}=0$. This corresponds to a single-site approximation, like the DMFA. In this case, the recoil momentum is absorbed in the unit cell at $\underline{R}=0$. The resulting expression for the nth-order contribution to the incoherent self-energy can then be evaluated analytically. The total self-energy is then found by performing the sum over n numerically.

The zero-temperature limit of the f quasiparticle self-energy for a metallic system is sketched in figure 4 for $\bar{n}=2$ and 4, where we have assumed an Einstein spectrum with $\hbar\omega_E=0.01$ for a value of the band width $W=3$, and a hybridization of $V=1/3$. All energies are given in units of eV's. It should be noted that the effect of the coherent (i.e. the zeroth-order) term in the self-energy is qualitatively different from the incoherent (higher-order) terms in that it expresses the coherent mixing of the f and d quasiparticle bands and is responsible for the level repulsion that produces the hybridization gap. The magnitude of the coherent hybridization is reduced as $\bar{n}$ is increased. At $T=0$, the sum of the incoherent terms resembles a coarse grained version of the standard electron–phonon self-energy [21] but is expected to be smoother if we use a continuous spectrum as in the Debye model. The imaginary part of the incoherent $T=0$ self-energy falls reasonably smoothly to zero in a frequency region of a width $\bar{n}\omega_E$ about the Fermi energy and saturates near $\pi V^2/W$ at higher-excitation energies (of the order of $\bar{n}\hbar\omega_E$). The value of the scattering rate at these high energies implies that the f levels are incoherent and behaving as independent atomic scatterers since the result is similar to that found at high energies for the single-impurity Anderson model. The unrenormalized nature of the high-energy limit of the scattering rate has been previously noted by Yang *et al* in the context of the anomalous phonon spectrum found in alpha-uranium [22, 23]. The incoherent contributions to the real part of the self-energy shows an approximate linear variation in the same frequency interval around the Fermi energy where the imaginary part exhibits the minimum. The linear ω-variation of the incoherent part of the self-energy contributes a factor of

$$Z^{\rm inc}=\left(1-\frac{\partial\Sigma_{\rm f}^{\rm inc}}{\partial\hbar\omega}\right)\bigg|_{\omega=0} \tag{17}$$

to the $T=0$ quasiparticle mass enhancement. The total enhancement of the $T=0$ quasiparticle mass is then given by the product

$$Z^{\rm inc}\exp\left[\frac{1}{N}\sum_{\underline{q}}\left(\frac{\lambda_{\underline{q}}}{\hbar\omega_{\underline{q}}}\right)^2\right]. \tag{18}$$

The inverse of this product is responsible for the renormalization of the hybridization gap at $T=0$ and also represents the many-body reduction of the quasiparticle weight in the complete f electron excitation spectrum. As the temperature is increased, the self-energies become smoother functions of ω. Also, as T increases, the value of $\bar{n}$ increases and, therefore, (due to the sum rule) the ratio of the incoherent to the coherent parts of the self-energy increases. Furthermore, the value of the imaginary part of the self-energy at the Fermi energy ($\omega=0$) increases as T is increased. At temperatures of the order of $\hbar\omega_E$, the temperature dependence of the imaginary part of the incoherent self-energy is controlled by the Bose–Einstein distribution function $N(\omega_E)$ and may be approximated by

$$\mathrm{Im}\,\Sigma_{\rm f}^{\rm inc}(\underline{k},0)=\frac{\pi|V_*|^2}{W}\sum_{n=1}^{\infty}\frac{(\frac{\lambda_E}{\hbar\omega_E})^{4n}}{n!n!}\times[1+N(\omega_E)]^nN^n(\omega_E) \tag{19}$$

where λ_E^2 represents the average of the squared electron–boson coupling strength.

5. Discussion

The hybridization gap can be inferred directly from inspection of the f quasiparticle Green's function. The k-resolved f quasiparticle density of states $A_{\rm f}(k,\omega)$ for the $T=0$ limit of our model is shown in figure 5. It is seen that the f quasiparticle spectra fall to zero at the excitation energy corresponding to the conduction band energy ϵ_k, as expected from a Fano anti-resonance. The broad portion of the f peak has a width of the order of $\pi|V|^2/W$. Furthermore, as $\bar{n}$ increases, the narrow quasiparticle peak moves closer to the Fermi energy, as is consistent with the closing of the hybridization gap. To be

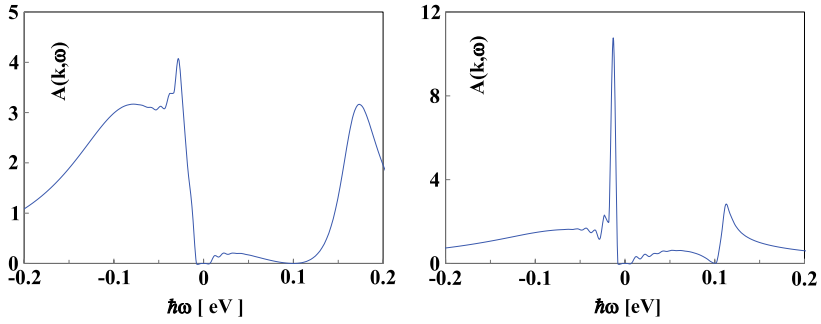

Figure 5. The frequency dependence of the zero-temperature limit of the k-resolved f quasiparticle density of states at $\epsilon_k - \mu = 0.1$ for $\bar{n} = 2$ (left panel) and for $\bar{n} = 4$ (right panel). For this case, the system is metallic as the Fermi energy lies at the edge of the hybridization gap. The spectra were calculated for the parameter values given by $\hbar\omega_E = 0.01$, $E_\mathrm{f} = -0.02$, $V = 1/3$ and $W = 3$ eV.

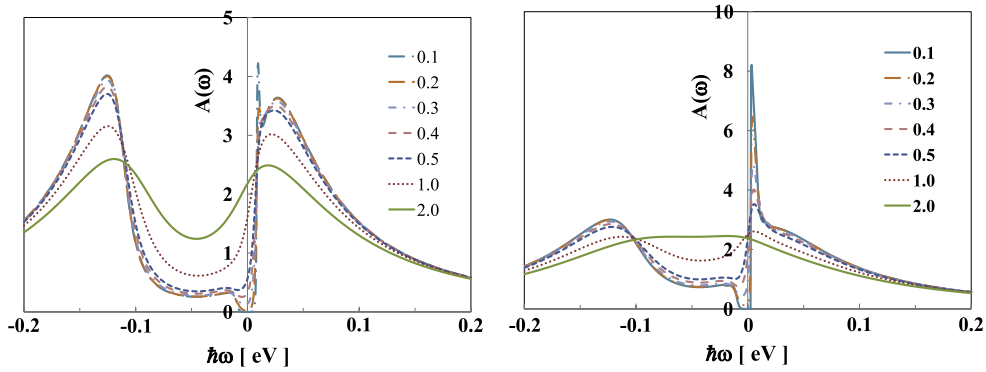

Figure 6. The f quasiparticle density of states for the various temperatures (given in the text). The left panel shows the results for $\bar{n} = 0.1$ and the right panel shows the results for $\bar{n} = 0.25$. It is seen that the low-excitation energy quasiparticle peak decreases rapidly as T first increases and then spectral weight starts growing in the gap region at higher temperatures. The values of the parameters chosen correspond to $\hbar\omega_E = 0.01$, $E_\mathrm{f} = -0.05$, $V = 1/3$ and $W = 3$ eV.

able to identify the hybridization gap more clearly, we shall examine the total f quasiparticle density of states. The f quasiparticle density of states can be expressed as

$$A_\mathrm{f}(\omega) = \frac{1}{\pi}\,\mathrm{Im}\left[\hbar\omega - E_\mathrm{f} + \mu - \Sigma_\mathrm{f}^{\mathrm{inc}}(\omega)\right]^{-1} + \frac{1}{\pi}\,\mathrm{Im}\left[\frac{{V_*}^2}{[\hbar\omega - E_\mathrm{f} + \mu - \Sigma_\mathrm{f}^{\mathrm{inc}}(\omega)]^2}F(\omega)\right] \tag{20}$$

where the complex function $F(\omega)$ is given by the integral

$$F(\omega) = \int_{-\infty}^{\infty} \mathrm{d}\epsilon\, \rho(\epsilon)\left[\hbar\omega - \epsilon + \mu - \frac{{V_*}^2}{\hbar\omega - E_\mathrm{f} + \mu - \Sigma_\mathrm{f}^{\mathrm{inc}}(\omega)}\right]^{-1} \tag{21}$$

and $\rho(\epsilon)$ is the conduction band density of states. The first term in $A_\mathrm{f}(\omega)$ represents the incoherent part of the f quasiparticle density of states. It has the exact form of the f electron Green's function for a single-site-impurity model. The second term represents the coherent part which reflects the hybridized band structure. Specifically, in the limit of a zero electron–boson interaction, the contribution to the density of states from the simple pole in the incoherent spectrum is precisely canceled by a corresponding factor in the coherent part, and the remaining terms of the coherent part yield the hybridized band structure. It is seen that, in the metallic case, the incoherent contribution dominates the spectra for large values of the electron–boson coupling and that the hybridization gap in the density of states is only observable as a pseudogap for small values of the electron–boson interaction. This is consistent with the observation that most systems with hybridization gaps show only modest mass enhancements. The f quasiparticle density of states are shown in figure 6 for the temperatures $k_\mathrm{B}T/\hbar\omega_E = 2, 1, 0.5, 0.4, 0.3, 0.2, 0.1$ and values of $\bar{n} = 0.1$ and 0.25. It is noted that as $\bar{n}$ increases, the weight of the narrow peak at the Fermi energy increases, and the spectral weight in the region of the hybridization gap structure increases. Furthermore, the temperature scale which controls the intensity of the Fermi energy peak is much smaller that the temperature scale at which the hybridization pseudogap closes (the latter temperature scale is of the order of $\hbar\omega_E$).

Although the shape of the f quasiparticle spectrum cannot be directly compared with the results of ARPES measurements, the temperature dependence of the hybridization gap can. ARPES measurements on UPd_2Al_3 were performed at the Synchrotron Radiation Center, Stoughton, WI on the PGM beamline. A Scienta4000 hemispherical analyzer was used with the energy resolution set to 15 meV and a photon energy 34 eV. The sample was cleaved in vacuum at high temperatures

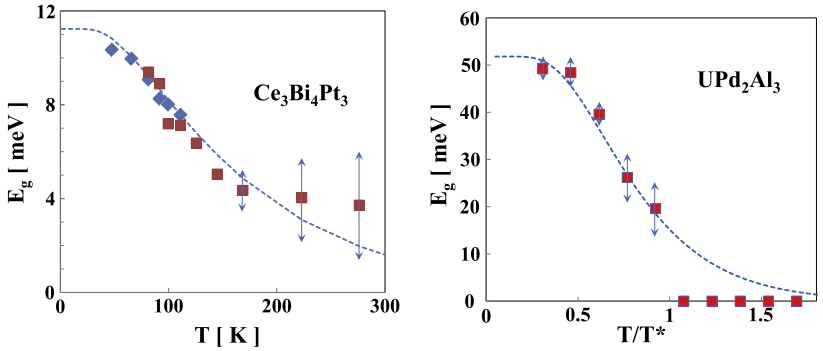

Figure 7. Left: the temperature dependence of the hybridization gap E_g inferred from transport measurements on the semiconducting material $Ce_3Bi_4Pt_3$ [14]. Right: the temperature evolution of the hybridization gap in metallic UPd_2Al_3.

and then cooled down while the photoemission spectra were collected. The temperature evolution of the hybridization gap (see figure 7) was extracted from the measured spectra by a numerical fitting procedure. A coherence temperature T^* of 65 K was found, which is directly related to the formation of the quasiparticle weight and the onset of the hybridization gap, as can be seen in the right panel of figure 7. In contrast with the gap extracted from transport measurements on the semiconducting material $Ce_3Bi_4Pt_3$ [3] which shows a similarity to the results of this theory, the results on UPd_2Al_3 show a mean-field like temperature variation and are more consistent with a slave boson treatment in which the gap vanishes above T^*.

Acknowledgments

This work was supported by a grant from the US Department of Energy, Office of Basic Energy Sciences, Materials Science through award DEFG02-84ER45872. The SRC is supported by the NSF under Award No. DMR-0084402.

References

[1] Aeppli G and Fisk Z 1992 *Comments Condens. Matter Phys.* **16** 155
[2] Riseborough P S 2000 *Adv. Phys.* **49** 257–320
[3] Hundley M F, Canfield P C, Thompson J D, Fisk Z and Lawrence J M 1990 *Phys. Rev.* B **42** 6842–5
[4] Breuer K, Messerli S, Purdie D, Garnier M, Hengsberger M, Panaccione G, Baer Y, Takahashi T, Yoshii S, Kasaya M, Katoh K and Takabatake T 1998 *Europhys. Lett.* **41** 565–70
[5] Riseborough P S 1998 *Phys. Rev.* B **58** 15534–47
[6] Severing A, Thompson J D, Canfield P C, Fisk Z and Riseborough P S 1991 *Phys. Rev.* B **44** 6832–7
[7] Riseborough P S 1992 *Phys. Rev.* B **45** 13984–95
[8] Bucher B, Schlesinger Z, Canfield P C and Fisk Z 1994 *Phys. Rev. Lett.* **72** 522–5
[9] Riseborough P S 1994 *Physica* B **199/200** 466
[10] Dordevic S V, Basov D N, Dilley N R, Bauer E D and Maple M B 2001 *Phys. Rev. Lett.* **86** 684–7
[11] Izawa K, Suzuki T, Fujita T, Takabatake T, Nakamoto G, Fujii H and Maezawa K 1999 *Phys. Rev.* B **59** 2599–603
[12] Ikeda H and Miyake K 1996 *J. Phys. Soc. Japan* **65** 1769–81
[13] Moreno J and Coleman P 2000 *Phys. Rev. Lett.* **84** 342–5
[14] Hundley M F, Thompson J D, Canfield P C and Fisk Z 1994 *Physica* B **199** 443–4
[15] Bonn D A, Garrett J D and Timusk T 1988 *Phys. Rev. Lett.* **61** 1305–8
[16] Donovan S, Schwartz A and Grüner G 1997 *Phys. Rev. Lett.* **79** 1401–4
[17] Lee T D, Low F E and Pines D 1953 *Phys. Rev.* **90** 297
[18] Sherrington D S and Riseborough P S 1976 *J. Phys. Colloq.* **37** C4 255–9
[19] Sherrington D S and von Molnar S 1975 *Solid State Commun.* **16** 1347
[20] Holstein T 1959 *Ann. Phys., NY* **8** 325
Holstein T 1959 *Ann. Phys., NY* **8** 343
[21] Engelsberg S and Schrieffer J R 1963 *Phys. Rev.* **131** 993
[22] Riseborough P S and Yang X-D 2007 *J. Magn. Magn. Mater.* **310** 938–40
[23] Riseborough P S and Yang X-D 2010 *Phys. Rev.* B **82** 094303